Blooming effects in indium antimonide focal plane arrays

I. Szafranek, O. Amir, Z. Calahorra, A. Adin, and D. Cohen
Semiconductor Devices (SCD), P.O. Box 2250, Haifa 31021, Israel

ABSTRACT

Studies of blooming effects in InSb focal plane array (FPA) detectors, are presented. Two blooming test devices are described, which have allowed to isolate optical, charge-diffusion and electronic blooming mechanisms. It is demonstrated that when a spurious illumination due to optical scattering is eliminated, then no extended blooming occurs, and only normal cross-talk mechanisms cause signal offset in elements adjacent to the hot target image. Cross-talk data are analyzed in terms of the signal decay versus element position, and the lateral carrier diffusion length is derived. Susceptibility of different diode structures to blooming, is discussed. It is also shown that an FPA signal processor may cause an extensive electronic blooming.

Keywords: Focal Plane Array, FPA, InSb detectors, IR detectors, blooming, cross-talk

1. INTRODUCTION

Until recently, thermal imaging systems have been primarily based on linear mercury cadmium telluride detectors operating in the 8÷12 μm spectral range (LWIR). High thermal flux in this range more than compensates for short integration times of < 100 μsec, which are available with scanning optics, thus allowing for a nearly background-limited operation.

New generation, two-dimensional (2-D) staring arrays provide much longer integration times of a few milliseconds. Therefore, with high quantum efficiency detectors, e.g., InSb 2-D Focal Plane Array (FPA), outstanding responsivity and detectivity are attainable even under relatively low-flux conditions, such as for typical earth ambient at 3÷5 μm range (MWIR). These FPA detectors gain overwhelming popularity, particularly considering that in addition to excellent radiometric characteristics the corresponding thermal imaging systems can have a more compact design, benefit of a better optics performance-to-weight ratio, and are potentially less expensive in high volume production.

However, already in early field tests of commercially available thermal cameras based on both InSb and PtSi FPA detectors, a predominant blooming effect has been observed, when targets at temperatures above a few hundreds degrees centigrade were present in the field of view. Blooming is defined as a partial or complete blinding of an FPA detector, due to uncontrolled spreading out of the signal from a hot target across large sections of the FPA. This effect, although not much publicized so far, is now widely recognized as a major potential drawback of the MWIR 2-D FPA systems, especially for demanding applications, where very hot extended objects are expected in a scene. The fact that blooming has not been observed to such a devastating extent in the conventional LWIR thermal imaging systems, has to be related not only to the differences in the relevant system designs, but also to the inherent radiometric properties of the two spectral bands. The radiance power span between hot target and background for typically required temperature difference of >1000 °C, is larger in MWIR compared to LWIR by more than two orders of magnitude. Frequently, this higher contrast in the MWIR range is considered as an advantage. However, in the context of blooming it means that spurious fractions of the hot target signal can easily saturate elements in the MWIR FPA detector.

In general, two types of blooming effects can be distinguished, namely local and global. The former originates in a normal cross-talk in the InSb and Si MUX chips, and therefore affects the target image vicinity only. It is the global blooming that is of a major concern. It can be attributed to both the optically dispersed irradiance and the CMOS signal processor malfunction. In order to isolate different blooming mechanisms, two special test devices have been studied. In this paper we demonstrate that ***in properly designed*** InSb 2-D FPA detectors the global blooming is primarily caused by radiation scattering in the optics outside the FPA. Photogenerated carriers in the back-illuminated, thin InSb chip cause saturation of elements only in the immediate neighbourhood of the legitimate hot target image. Ideally, the extent of this saturation is charge diffusion-limited, and therefore depends on InSb element design and process characteristics. It is also shown that in a signal processor with a limited current throughput capability, an extended hot target can cause a voltage offset and, possibly, even saturation in the output buffer of the FPA, thereby leading to a global electronic blooming.

2. EXPERIMENTAL

Two designated test chips were studied, as described below:

2.1 Test Chip #1

This device is a modified 128×128 InSb FPA prototype, originally developed at SCD in 1995. The InSb chip was divided into four equal quadrants, each with a different type of diodes, schematically described in Figure 1. Both the back, illuminated InSb interface and the edges of the encapsulated gap between the InSb and Si MUX chips, were coated with an opaque gold layer, which had a small clear aperture in its center, as shown in Figure 2.

The hot target image was generated by focusing on the FPA a ∅2 cm orifice of a cavity blackbody at ~1100 °C. A commercial f/2 IR optics and a 3÷5 μm bandpass cold filter, were used. The orifice image of about 15 pixels in diameter was obtained, as shown in Figure 3-a and discussed later. The image could be moved around the focal plane. Images were also taken with the hot orifice outside the field of view. The whole experiment was video-taped. Specific images were stored in a computer for further quantitative analysis.

In order to enable various saturation levels in both the illuminated and the dark regions of the FPA, the integration time was varied over the range of $5\times10^{-7} \div 1$ sec. Each measurement of the blackbody orifice image was accompanied by reference data with the orifice blocked, so that the net cross-talk and blooming contribution could be evaluated by computing differential images.

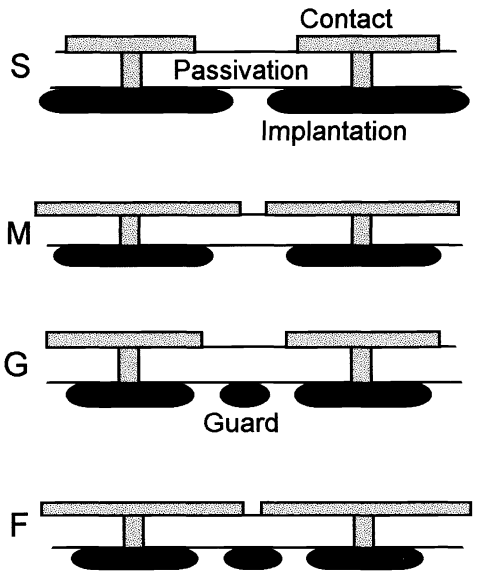

Figure 1: Four different diode types included in the FPA blooming Test Chip #1.

Cross-talk and blooming effects were investigated by imaging the hot orifice on the clear aperture boundary in different quadrants. The external optical blooming accounted for the signal expansion across the directly illuminated clear aperture area. Since the signal in the coated area could not be affected by any scattered illumination, it was purely due to the dark current of the detector, plus a cross-talk from the illuminated zone. Thus, in this area both localized charge diffusion cross-talk and global electronic blooming along illuminated FPA columns, were observed with high sensitivity. The local effect was quantitatively analyzed as a function of a specific diode structure, as well.

Various measurements discussed in the next section, are summarized in Table 1.

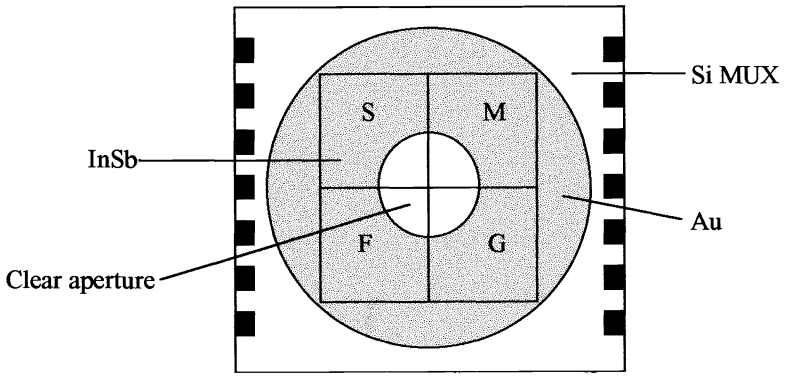

Figure 2: Schematic design of the FPA Test Chip #1 used to study both local and global blooming effects.

Table 1: Summary of the main measurements discussed in the text.

File (Figure #)	Integration Time [msec]	Hot Spot Image Location	Remarks
a1 (Fig. 3-a)	0.001	Aperture boundary in the S-zone.	Hot spot at ~50% saturation.
a4 (Fig. 3-b)	1.0	Same as above.	297K background in the clear aperture at ~50% saturation.
d2 (Fig. 3-c)	10	Same as above.	Coated S elements at ~50% saturation.
d1	10	None	Reference file.
e2	0.2	Aperture boundary, across the M and G zones.	Compares blooming in guarded versus unguarded diodes.
e1	0.2	None	Reference file.

2.2 Test Chip #2

Two separate Built-In-Test (BIT) circuits have been incorporated in the CMOS signal processor, which was developed for SCD's 320×256 InSb FPA in 1996. They enable direct injection of current at two independent levels into different FPA areas. One of these circuits is a designated electronic blooming BIT circuit, which controls the input signal to a subarray of 32×40 elements in the signal processor, bordered by rows 65÷96 and columns 281÷320. For electronic blooming tests, a high current of the order of 10 μA/element was injected into this area. The remaining elements, which are connected to the second BIT circuit, may simultaneously receive either no current at all, or a low current of ~1 nA, typical of 300K background level. Any signal increase in these elements when the high-current BIT is activated, provides a direct measure of the electronic cross-talk and blooming inherent in our CMOS design.

3. RESULTS AND DISCUSSION

3.1 Electro-optical cross-talk and blooming

Images of the hot blackbody focused on the border between illuminated and covered regions in the S-zone of the Test Chip #1, are shown in Figure 3 for three different integration times (T_{INT}). Figure 3-a was taken with the shortest integration time of 0.001 msec. In the hot spot area, the detector elements are at about 50% saturation level. Considering integration capacity of ~17×10^6 electrons, the photoelectric current was estimated at about 1.3 μA. Practically no signal is detected with this short integration time in the remaining sections of the FPA.

The image in Figure 3-b was taken with T_{INT} = 1 msec, which corresponds to about 50% saturation in the unmasked S-type elements at ~297K background. The high signal region, shown by the darker gray level, expands all over the S and into M and F quadrants in the clear aperture area. This is a typical example of the optical blooming due to scattering of the hot target irradiance, which has been observed in commercial MWIR staring imaging systems. Again, practically no signal is detected in the covered area.

Finally, an image taken with the longest integration time of 10 msec, is shown in Figure 3-c. The whole clear aperture becomes now saturated, while in the coated region four distinct zones are observed, each comprising of the different diode structure with its characteristic dark current. It should be noted that even with this long integration time, no anomalous strong signal can be detected in the coated area away from the directly illuminated clear aperture.

For a more detailed observation of the blackbody illumination effects, the difference of the image files (d2-d1) is given in Figure 4. File (d2) is the one shown in Figure 3-c. File (d1) was recorded using the same integration time, but with the blackbody opening blocked (see Table 1). In both cases the central, illuminated zone is saturated under the ambient background. The image in Figure 4 represents the net changes in the coated areas because of the hot blackbody radiation. As can be qualitatively seen, both the lateral extent and the intensity of the blooming are negligible compared to those observed with commercial thermal imaging systems, and demonstrated here within the clear aperture area of the FPA in Figure 3-b. Moreover, two different effects are distinguished:

- **Local** - a signal increase in the S-type elements adjacent to the clear aperture boundary;
- **Global** - a uniform signal level increase in the S and F zones along the columns, which cross the hot spot image.

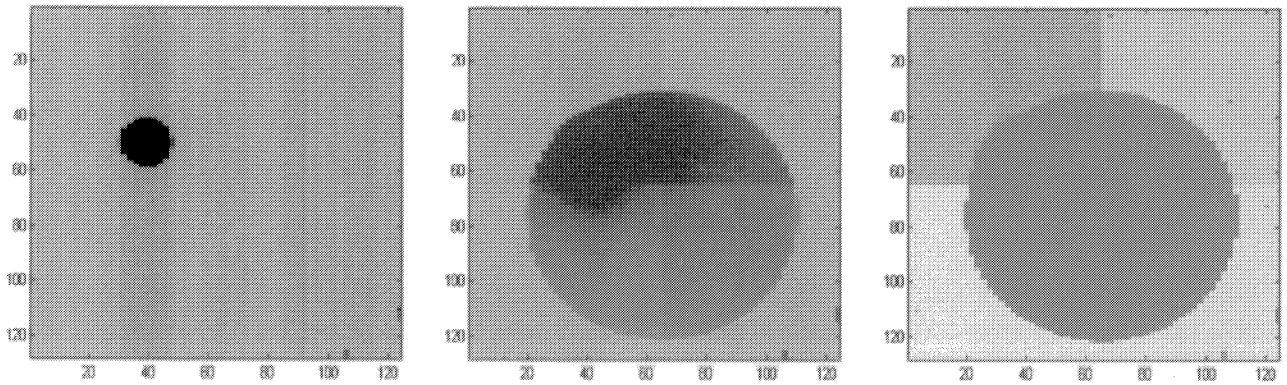

(a) **(b)** **(c)**

Figure 3: Thermal image of a 1100 °C cavity blackbody orifice taken with the 128×128 InSb FPA, as described in text. The integration times were: **(a)** 0.001 msec, **(b)** 1 msec, and **(c)** 10 msec. In all FPA images shown in Figures 3, 4 and 7, an arbitrary display scale of gray levels has been used.

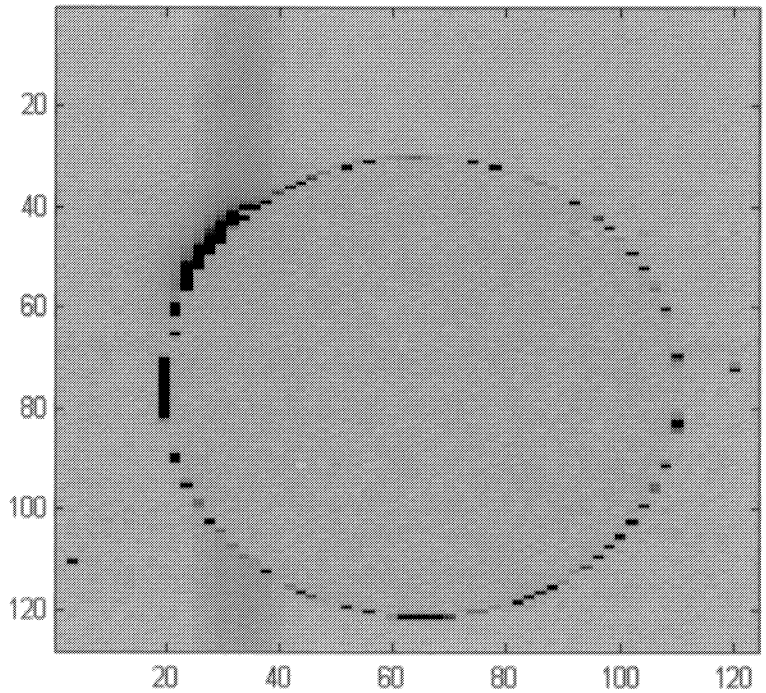

Figure 4: Signal difference of the image files (d2-d1), as defined in Table 1. Both the local cross-talk due to charge diffusion, and the global electronic blooming along columns 25÷40, which cross the hot spot image, are discernible.

In order to understand the nature of the local effect, the signal level variation along a row which crosses the hot spot, is depicted in Figure 5. In Figure 5-a the "+" and "o" marks represent files (d1) and (d2), respectively. In Figure 5-b the signal difference, (d2-d1), is plotted. On a semi-log scale it can be clearly seen, that the signal in the dark zone decays by an order of magnitude over the distance of about five pixels. It gives an estimate of the lateral diffusion distance, $L \approx 100$ μm. This dependence on distance is believed to originate in the normal cross-talk mechanism, namely the lateral diffusion of photogenerated charge carriers in the InSb chip. The cross-talk level in the next-nearest neighbour to the aperture boundary is estimated at $<5\times10^{-4}$ of the hot target signal.

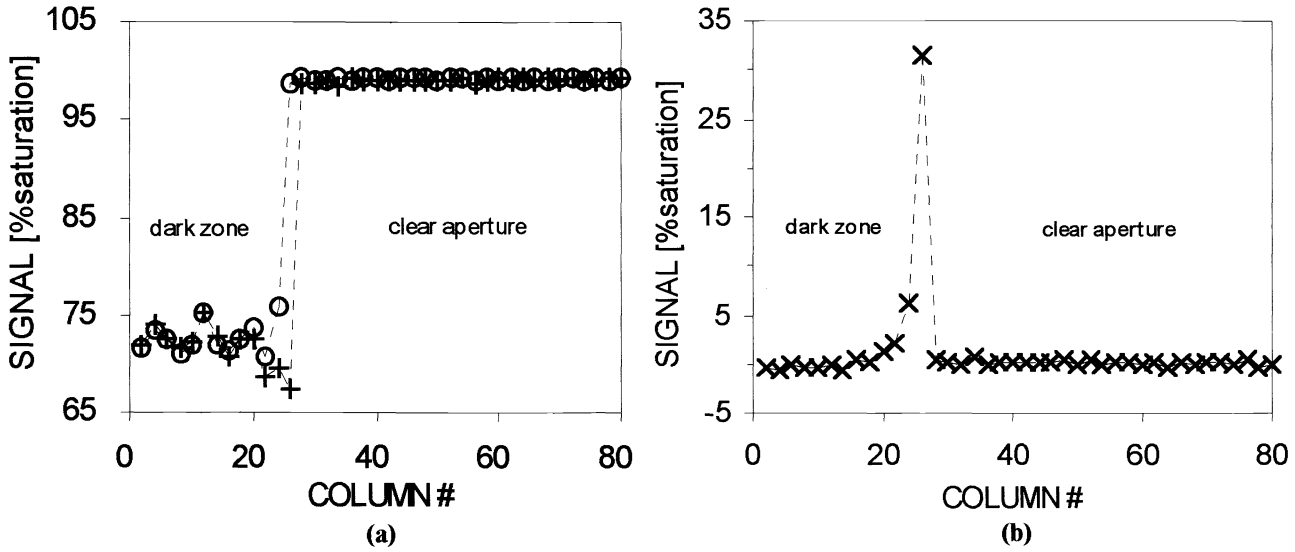

Figure 5: **(a)** Signal variation in elements along a ***row*** which contains the hot orifice image. "+" and "o" represent files (d1) and (d2), respectively, as defined in Table 1. **(b)** Signal difference of the image files (d2-d1) along this row. Only a local blooming effect is observed, which decays exponentially with distance from the aperture boundary.

The same behaviour is also observed along columns crossing the hot spot. However, in this case there is an additional dc offset of the signal, which extends uniformly along these columns at the level of about 1.5% saturation. This effect is shown in Figure 6 for the difference of images (d2-d1). In Figure 6-a the dc offset is seen to spread both to the left (i.e. upward from the hot spot in Figure 4), and far to the right, namely downward along the column, beyond the clear aperture. This wide lateral extent, independent of the actual hot spot location, gives rise to the definition of this effect as a global blooming. In this case it was caused by the signal processor electronics, as discussed in the following section. Figure 6-(b) provides a closer look at the local blooming along the column. As expected, it is similar to the cross-talk along the rows, but here the cross-talk signal decays only to the dc offset level generated by the global electronic effect.

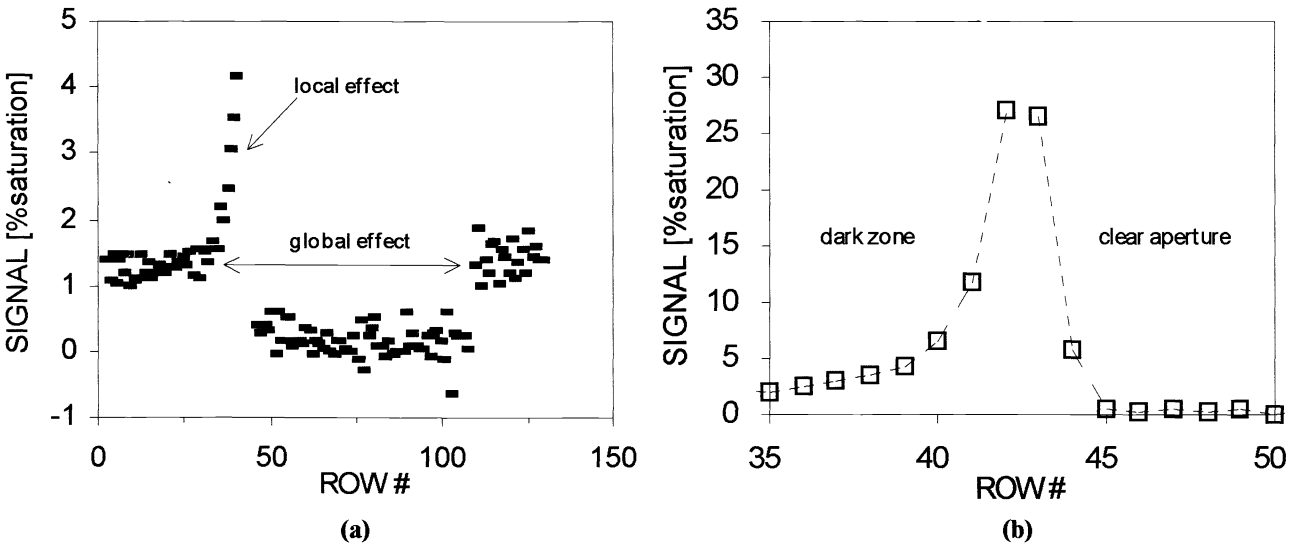

Figure 6: Signal difference of the image files (d2-d1) along a ***column*** crossing the hot spot image. **(a)** Both the global blooming caused by the signal processor and the localized cross-talk, are demonstrated. **(b)** Zoom view of the signal decay along this column in the coated area adjacent to the hot spot image.

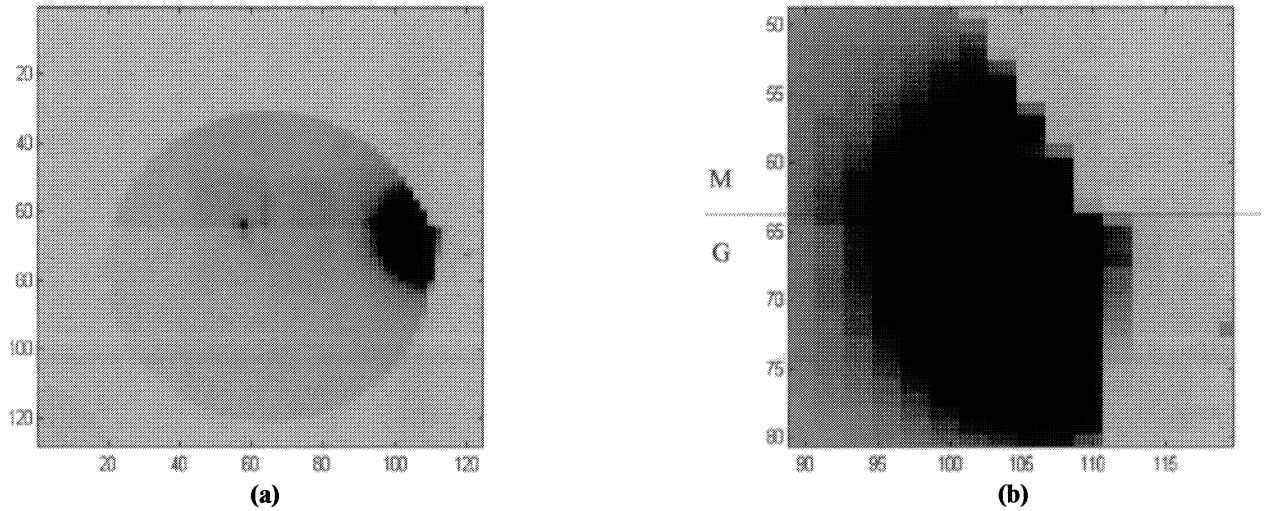

Figure 7: Signal difference of the image files (e2-e1). The hot spot is located on the borderline between the M and G-type diode zones. **(a)** Full FPA view; **(b)** Zoom on the spot area, showing a greater extent of the blooming in the G zone.

The extent of the local blooming depends on technological details, such as diode structure, InSb thickness and its surface passivation. By illuminating the various InSb quadrants in Test Chip #1, the effect of the diode structure on the local blooming was analyzed. An example is shown in Figure 7, which presents the difference of the image files (e2-e1), as defined in Table 1. The local cross-talk is much more extensive in the guarded G-type diodes. A plausible explanation is that the guard generates a significant photocurrent, which due to a finite resistance of the thinned InSb chip, leads to an offset in the reverse bias of the neighboring elements. It is quite fortunate that the S-type diodes, which represent the most desired FPA element structure from the point of view of the fill factor and quantum efficiency, are less susceptible to cross-talk and blooming, than the more evolved guarded diodes.

3.2. Electronic cross-talk and blooming

In principle, the following global electronic cross-talk and blooming mechanisms along columns have been identified in the particular signal processor design of the 128×128 FPA prototype, which served as a basis for Test Chip #1:

1. A voltage offset in all column elements due to a distributed column line resistance;
2. A voltage offset in all column elements due to a finite loop gain of the column output amplifier;
3. The amplifier saturation, when the total column current is higher than amplifier's overload limit (a few tens of μA).

As mentioned earlier, the electronic blooming shown in Figures 4 and 6 occurred, when a photoelectric current of ~1.3 μA/pixel was generated in about 15 elements in a column. Under these experimental conditions only the first two mechanisms were active. The corresponding signal offset was then proportional to the total current, which the column output amplifier had to absorb during the inter-frame reset period. The third effect is much more dramatic, eventually leading to the saturation of the entire column. However, it would appear at much higher photoelectric currents, and/or for larger extended hot targets in the field of view of the FPA detector.

The occurrence and the magnitude of these global blooming effects depend on a detailed design of the column line electronics. This design has been corrected and optimized for negligible cross-talk and blooming in the final versions of both 128×128 and 320×256 signal processors, which were developed at SCD in 1996. In order to experimentally confirm that the electronic blooming problem has been resolved, the designated BIT circuit has been incorporated in Test Chip #2 (see Section 2.2).

Figure 8 presents typical data measured on Test Chip #2. It shows the signal variation along row 90 and column 300, which cross the high-injection (Ibit = 10 μA) BIT area of 32×40 pixels. No current was injected into the second BIT circuit, which is connected to the remaining array elements. Any signal increase in these elements indicates electronic cross-talk from the active BIT region. Two data sets at T_{INT} = 2 msec and 20 msec, were collected. In both cases the high-injection BIT subarray was saturated. No dependence of the cross-talk on integration time has been observed.

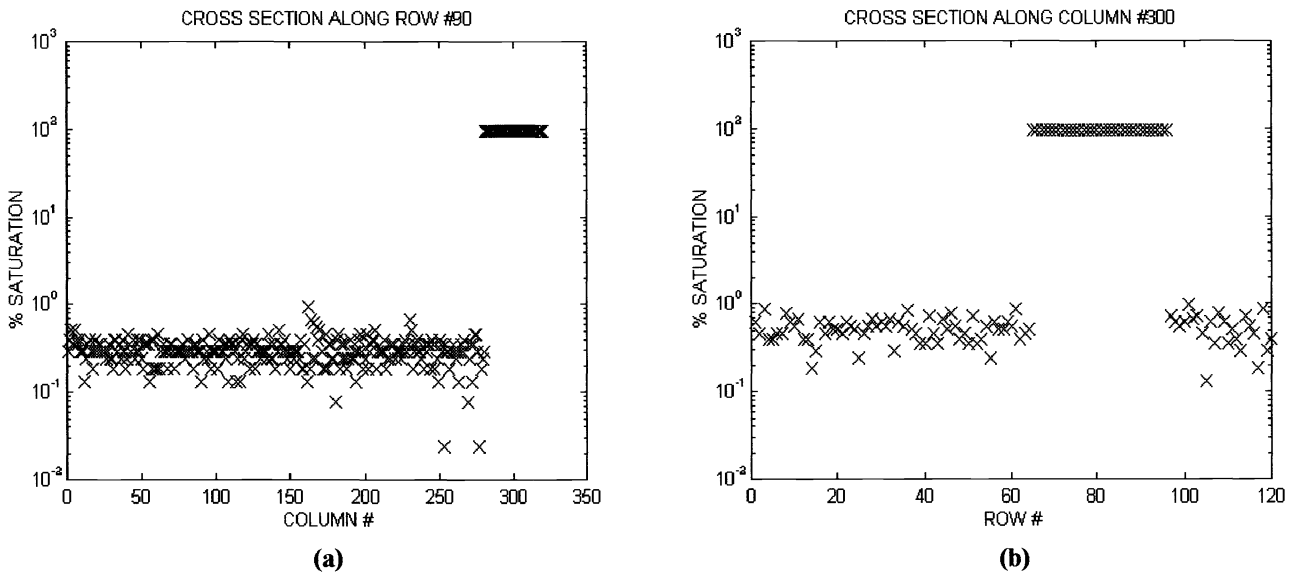

Figure 8: Signal variation in elements along: **(a)** row #90, and **(b)** column #300 in Test Chip #2. Ibit = 10 μA was injected into the 32×40 blooming BIT subarray, no BIT current in the remaining elements. Data for T_{INT} = 20 msec are shown. The signal offset because of an electronic blooming outside the high-injection BIT area, is negligible.

The signal measured in the Ibit = 0 area, including even elements immediately adjacent to the high-current BIT subarray, was only ~0.5% and ~0.3% of saturation along columns and rows, respectively. The latter measurement was actually noise-limited by the test equipment. Considering the extremely high BIT current used (10 μA/pixel, or $>10^4$ of the 300K background level) and a very large high-injection area, this electronic blooming level may be considered negligible for all practical purposes.

4. CONCLUSIONS

Two independent blooming effects should be distinguished in MWIR FPA detectors: local and global. The former is apparently associated with the lateral charge diffusion in InSb. It is similar to the regular electro-optical cross-talk, and therefore rather independent of the high flux conditions. Since the local blooming affects only the immediate vicinity of the legitimate hot target image, it should not degrade substantially the overall imaging performance of FPA detectors. For the utmost cross-talk localization, the sensing element structure, thinned InSb resistance and contact quality should all be carefully considered.

On the other hand, the global blooming may cause a signal offset or even saturation across wide portions of an FPA detector. Two such effects have been demonstrated and discussed: electronic and optical. The electronic blooming should not be of a concern in properly designed FPA signal processors, as shown here for the BIT blooming data of SCD's 320×256 CMOS MUX.

It is the optically dispersed irradiance, which under usual circumstances may cause a major interference to the image quality of MWIR FPA-based thermal imaging systems. Using commercially available collimating optics, this optical scattering effect has been clearly observed in the illuminated clear aperture of Test Chip #1, where under normal operating conditions ($T_{INT} \approx 1$ msec) the hot image expanded far away from the actual target image. On the other hand, it has been positively demonstrated that once the optical blooming is eliminated (in our case by covering parts of the FPA with the opaque gold coating), no extended image distortion occurs.

In conclusion, we have demonstrated that ***in properly designed*** InSb and CMOS signal processor components of 2-D FPA detectors, there should be no inherent blooming mechanisms of practical consequences. The widespread blooming disturbance, which is frequently discernible in MWIR FPA-based commercial imaging systems, may be caused by external optical effects. It is only by a stringent optical design, that these effects can be minimized to a practically acceptable level.